Development 133, 2731-2745 (2006) doi:10.1242/dev.02426

Neural tube derived signals and Fgf8 act antagonistically to specify eye versus mandibular arch muscles

Gudrun von Scheven, Lúcia E. Alvares*, Roy C. Mootoosamy† and Susanne Dietrich§

Recent knockout experiments in the mouse generated amazing craniofacial skeletal muscle phenotypes. Yet none of the genes could be placed into a molecular network, because the programme to control the development of muscles in the head is not known. Here we show that antagonistic signals from the neural tube and the branchial arches specify extraocular versus branchiomeric muscles. Moreover, we identified Fgf8 as the branchial arch derived signal. However, this molecule has an additional function in supporting the proliferative state of myoblasts, suppressing their differentiation, while a further branchial arch derived signal, namely Bmp7, is an overall negative regulator of head myogenesis.

KEY WORDS: Chick, Quail, Embryo, Head mesoderm, Skeletal muscles, Eye muscles, Lateral rectus, Branchiomeric muscles, Mandibular arch, Jaw muscles, *Lbx1*, *Paraxis*, *En2*, *Myf5*, *MyoR*, *Fgf8*, *Bmp7*

INTRODUCTION

Vertebrate skeletal muscles are the basis for all voluntary movements. However, while trunk muscles predominantly serve locomotion and the maintenance of body posture, this is not the purpose of muscles in the head. Here, muscles are used for food uptake, mastication and swallowing, for the control of the cranial openings and facial expression, for respiration in animals relying on gill breathing, and for the movement of the eyes. These, however, are crucial functions, and an impairment of craniofacial muscles is a threat to life (Goodrich, 1958).

Muscles in the head develop from two sources: the unsegmented para- and pre-otic head mesoderm, and post-otically, from segmented paraxial mesoderm, namely the occipital somites (Couly et al., 1992; Jacob et al., 1984; Noden, 1983a; Wachtler and Jacob, 1986). The occipital somites deliver the posterior pharyngeal and laryngeal muscles and the muscles of the tongue. They have been secondarily incorporated into the head during vertebrate evolution and largely develop like trunk somites (Gans and Northcutt, 1983). The unsegmented paraxial head mesoderm provides the muscles of the first three branchial arches, including the jaw closure muscles [first or mandibular arch muscles (MAM), innervated by the trigeminal nerve], the jaw opening and facial muscles (second or hyoid arch muscles, innervated by the facial nerve) and the anterior pharyngeal and laryngeal muscles (third branchial arch muscles, innervated by the glossopharyngeal nerve) (Couly et al., 1992; Jacob et al., 1984; Noden, 1983a; Wachtler and Jacob, 1986). Moreover, this mesoderm is the source of two of the extrinsic eye muscles [lateral rectus extraocular muscle (EOM), innervated by the abducens nerve, and dorsal oblique EOM, innervated by the trochlear nerve], while the remaining four EOM originate from prechordal head mesoderm (dorsal rectus, ventral rectus, medial rectus, ventral oblique EOM, all innervated by the oculomotor nerve). Most of the prechordal mesoderm joins the paraxial head mesoderm before muscle development, such that EOM and the muscles of the anterior branchial arches develop from a morphologically continuous strip of mesenchyme (Jacob et al., 1984; Wachtler and Jacob, 1986). Moreover, this mesenchyme has the same myogenic potential (this study). We thus will collectively refer to it as head mesoderm.

It was established only recently that the head mesoderm employs a distinct programme of myogenesis (Mootoosamy and Dietrich, 2002). Key regulators of somitic myogenesis such as *Pax3* are absent (Hacker and Guthrie, 1998; Mootoosamy and Dietrich, 2002). Moreover, signals that stimulate trunk muscle development suppress myogenic differentiation in the head (Tzahor et al., 2003). Myf5, the first muscle determining factor to be expressed in the embryo, employs distinct promoter and enhancer elements in the head and in the trunk (Hadchouel et al., 2000; Summerbell et al., 2000), while knockout mice for the two basic helix-loop-helix transcription factors MyoR and Capsulin (Lu et al., 2002), mice lacking the T-box gene *Tbx1* (Kelly et al., 2004), or mice lacking the homeobox gene *Pitx2* (Gage et al., 1999; Kitamura et al., 1999), display distinct craniofacial, but not trunk muscle, defects. However, neither the cascades that trigger the myogenic differentiation of the head mesoderm, nor the cascades that specify the individual head muscles, are known.

Classically, neural crest cells are thought to control the developing head muscles (Noden, 1983b). Neural crest cells provide the majority of skull bones, and in addition the connective tissue, tendons and muscle attachment points for muscles in the head (Couly et al., 1993; Köntges and Lumsden, 1996; Noden, 1983a). Moreover, they carry positional information, the alteration of which leads to patterning defects of both bone and muscle (Grammatopoulos et al., 2000; Noden, 1983b; Pasqualetti et al., 2000). In zebrafish neural crest cells in mutants such as *chinless*, and in human DiGeorge patients, head muscle is severely impaired (Kelly et al., 2004; Schilling et al., 1996). However, the candidate gene for DiGeorge syndrome, *Tbx1*, affects neural crest cells indirectly (Vitelli et al., 2002a; Vitelli et al., 2002b). Moreover, the gene is expressed in branchial arch muscle, and hence may influence muscle development directly (Kelly et al., 2004). In addition, in-vivo

King's College London, Department of Craniofacial Development, Floor 27 Guy's Tower, Guy's Hospital, London Bridge, London SE1 9RT, UK.

*Present address: Universidade Federal do Paraná – UFPR, Centro Politécnico, Jardim das Américas, Rua Coronel Francisco Hoffman dos Santos 100, Setor de Ciências Biológicas, Departamento de Biologia Celular, 3o Piso, Sala 201, 81531-980 Curitiba – PR, Brazil.
†Present address: King's College London, Wolfson Centre for Age Related Diseases, Wolfson Wing, Hodgkin Building, Guy's Campus, London SE1 1UL, UK.
§Author for correspondence (e-mail: susanne.dietrich@kcl.ac.uk)

Accepted 3 May 2006

and in-vitro studies led to conflicting results regarding the requirement of neural crest cells for muscle differentiation; thus the role of these cells remains unclear (Tzahor et al., 2003).

Besides neural crest cells, the structures targeted by head muscles are also suspected to control craniofacial myogenesis. For example, in *ZRDCT-An* anophthalmic mouse mutants lacking eyes, eye muscles are severely reduced (Paterson and Kaiserman-Abramof, 1981). Likewise, in eyeless hagfishes, no eye muscles are found, a remarkable exception to the otherwise stereotype arrangement of eye muscles in vertebrates (http://tolweb.org/tree?group=Hyperotreti&contgroup=Craniata) (Brodal and Ragnar, 1963). However, hagfishes, which constitute a sister group to lampreys, have highly specialised life styles and may have secondarily lost their eyes and eye muscles. Thus, it remains open whether head muscle development requires the presence of muscle targets.

Finally, the innervating nerves have been thought to control muscle development in the head. In patients suffering from Duane's syndrome, the abducens nerve fails to innervate the lateral rectus EOM, which either degenerates or survives when misinnervated by the oculomotor nerve (Engle, 2002). In a similar vein, in patients suffering from fibrosis of extraocular muscles (FEOM) type2, trochlear and oculomotor-innervated muscles fail, as these nerves are absent (Nakano et al., 2001). However, in animal models for Duane's and FEOM type2, muscle anlagen first develop, suggesting that innervation may not be required for the initial steps of muscle development (Engle, 2002).

Conceptually, muscles that develop from head mesoderm can be organised into two groups, the EOM and the branchiomeric muscles. EOM develop from the more anterior and medial aspect of the head mesoderm and remain outside the branchial arches at all times (Couly et al., 1992; Noden, 1983a; Wachtler and Jacob, 1986). Motor neurons innervating these muscles resemble somatic motor neurons in the trunk (Jacob et al., 2001). The branchiomeric muscles arise from the more posterior and lateral aspect of the head mesoderm and develop within the branchial arches (Couly et al., 1992; Noden, 1983a; Wachtler and Jacob, 1986). Their motoneurons resemble visceral motoneurons (Jacob et al., 2001). Notably, branchiomeric muscle precursors express *MyoR* and *Capsulin* before *Myf5* (von Scheven et al., 2006).

At the level of the anterior hindbrain, precursors for prospective eye and branchiomeric muscles sit side by side as the anlage of the lateral rectus EOM is medially adjacent to developing MAM (Couly et al., 1992; Noden, 1983a; Wachtler and Jacob, 1986). Here, muscles express additional markers, with *Paraxis* and *Lbx1* characterising the EOM (Mootoosamy and Dietrich, 2002) and *En2* labelling the MAM (Gardner and Barald, 1992). Thus, focusing on this territory, we have the tools to simultaneously address the differentiation and specification of eye versus branchiomeric muscles.

Using heterotopic transplantation in the chick embryo, we first established that the head mesoderm develops into muscle according to localised, extrinsic cues. Ablation experiments then revealed that neural crest cells, the eye as the ultimate EOM target, or the innervating nerves do not control the onset of muscle differentiation or muscle specification. However, the neural tube provides a signal that specifies the lateral rectus EOM. This signal is anteroposteriorly unrestricted, soluble and acts in conjuction with a further, unidentified cue. In its absence, while muscle differentiation continued, the muscle anlage erroneously expressed the MAM marker *En2*. Moreover, the abducens nerve fell short of its target. This suggests that the neural tube supports the specification of EOM and suppresses the specification of arch muscles, in order to aid eye-muscle innervation.

The upregulation of *En2* upon separation of head mesoderm and neural tube suggested that branchial arch derived signals might stimulate MAM and suppress EOM development. Implanting beads loaded with signalling molecules expressed in the brachial arches, we found that Bmp7 had a generalised, negative effect on head muscle development. Fgf8, however, displayed a dual function: it upregulated *En2* expression and suppressed *Paraxis* expression, indicating that it antagonises the neural tube derived signals and supports MAM against EOM development. In addition, Fgf8 upregulated *MyoR*, a marker for proliferative, undifferentiated arch muscle precursors, and suppressed *Myf5*, indicating that Fgf8 controls muscle precursor proliferation versus differentiation.

MATERIALS AND METHODS

Chick and quail embryos

Fertilised hens' and quails' eggs were obtained from Winter Farm (Royston) and Potter Farm (Woodhurst), and incubated at 38.5°C in a humidified incubator. Embryos were staged according to (Hamburger and Hamilton, 1951).

Protein-loaded beads

Recombinant human Fgf4 or Fgf8 (R&D) at 500 μg/ml or 100 μg/ml was loaded onto Heparin-Acrylic beads (Sigma) as described by Alvares et al. (Alvares et al., 2003). Recombinant human Bmp2, Bmp4 or Bmp7 (R&D) at 500 μg/ml or 100 μg/ml and Shh (R&D) at 100 μg/ml was loaded onto Affi-Gel blue agarose beads (Biorad) as described in Dietrich et al. (Dietrich et al., 1998).

Tissue culture cell implants

Rat B1 control cells and cells expressing Wnt1 were raised, labelled with Celltracker Orange (Molecular Probes), aggregated and implanted as described in Cheng et al. (Cheng et al., 2004).

Microsurgery

In ovo microsurgery was carried out with flame-sharpened 100-μm tungsten needles as described previously (Alvares et al., 2003; Dietrich et al., 1998; Dietrich et al., 1997; Mootoosamy and Dietrich, 2002). Cranial operations were performed at HH10, before head muscle development and innervation (Noden et al., 1999). The exceptions were neural crest ablations and the heterotopic transplantation of head mesoderm fragments, which were carried out at HH8-9^{-}, before the emigration of cranial neural crest cells (Lumsden et al., 1991). Barrier experiments were performed using 7.5-μm-thick tantalum foil [Goodfellow; (Dietrich et al., 1998; Dietrich et al., 1997)], filter experiments using 25-μm-thick polycarbonate filters with a pore size of 0.05 μm [Costar; (Fan and Tessier-Lavigne, 1994)]. Operations at flank levels were performed at HH16 as described by Lours and Dietrich (Lours and Dietrich, 2005); the mid-hindbrain neural tube grafts were derived from HH10 donors. After surgery, the eggs were incubated for 48 hours, then harvested and fixed as outlined above.

Electroporation

The pCAβ-IRES-eGFP vector described in Alvares et al. (Alvares et al., 2003) or this vector harbouring the open reading frame of mouse *Hoxb1* (Bell et al., 1999) was injected into the HH10 neural tube at midbrain-hindbrain levels and electroporated as described in Schubert and Lumsden (Schubert and Lumsden, 2005).

In-situ hybridisation

Whole-mount in-situ hybridisation was carried out as previously described (Dietrich et al., 1998; Dietrich et al., 1997; Mootoosamy and Dietrich, 2002). Probes and their expression patterns are detailed in the following references: *Bmp7* (Begbie et al., 1999); *Dlx5* (Ferrari et al., 1995); *En2* (Logan et al., 1992); *Fgf8* (Mahmood et al., 1995); *Lbx1* (Dietrich et al., 1998); *Myf5* (Saitoh et al., 1993); *MyoR* (von Scheven et al., 2006); *Paraxis* (Sosic et al., 1997); *Shh* (Johnson et al., 1994).

Immunohistochemistry

Upon in-situ hybridisation, whole-mount immunohistochemistry was carried out according to Guthrie and Lumsden (Guthrie and Lumsden, 1992). Axonal staining was performed using the RMO270 antibody (Zymed; dilution 1:3000), which recognises the 155-kDa intermediate neurofilament subunit. Quail tissues were identified using the QCPN antibody (Developmental Studies Hybridoma Bank, University of Iowa, IA; dilution 1:200), the developing eye using a Pax6 antibody (Developmental Studies Hybridoma Bank, University of Iowa, IA; dilution 1:200), and eGFP protein using an anti-eGFP antibody (Molecular probes; dilution 1:2000). In all cases, signals were detected using anti-mouse IgG conjugated with horseradish peroxidase (Dako; dilution 1:100) and a peroxidase substrate kit (Vector Laboratories).

Sectioning

Embryos were embedded in 20% gelatin (Sigma) in PBS at 50°C, then cooled to 4°C. Subsequently, blocks were trimmed and fixed in 4% PFA for up to 2 days, then rinsed in PBS and sectioned to 50 μm on a Pelco 1000 Vibratome. Sections were collected on gelatinised slides and mounted in either 80% glycerol/PBS, or Aquamount (BDH).

Photomicroscopy

After in-situ hybridisation and/or immunohistochemistry, embryos were cleared in 80% glycerol/PBS. Whole-mounted embryos were split mid-sagitally before analysis. Embryos and sections were photographed on a Zeiss Axiophot, using Nomarski optics.

RESULTS

Heterotopic grafting of head mesoderm

We recently showed that in the trunk, limb muscle precursors possess positional information that predisposes them towards the programme for migratory muscle precursor formation (Alvares et al., 2003). Fate mapping experiments for the head mesoderm have established that EOM and the muscles of the first three branchial arches develop from distinct regions (Couly et al., 1992; Noden, 1983a; Wachtler and Jacob, 1986). Moreover, the head mesoderm can superimpose its identity on individuated neural crest cells (Trainor and Krumlauf, 2000). We thus investigated whether the localised formation of muscle anlagen in the head depends on intrinsic or extrinsic cues.

Heterotopic grafting of head mesoderm fragments was carried out on the right side of embryos as indicated in Fig. 1A, using quail donors and stage-matched chicken hosts. The operations were performed before neural crest cell emigration at HH8-9⁻, as neural crest cells have been suggested to provide positional information and patterning cues for the developing muscles (Noden, 1983b). As a control, head mesoderm at the level of the anterior hindbrain was grafted orthotopically.

The grafted tissue was traced using the QCPN antibody (Fig. 1B-H, brown staining). The specification of the lateral rectus EOM was investigated using *Paraxis* (not shown) and *Lbx1* (Fig. 1B-F, blue staining) as markers; both markers gave identical results. The position of all muscle anlagen was examined, assaying for the expression of the muscle-determining factor *Myf5* (Fig. 1G,H, blue staining). The embryos were analysed 48 hours post-surgery at HH19, as all markers are robustly expressed at this stage (Mootoosamy and Dietrich, 2002).

When head mesoderm from rhombomere 2 levels was grafted orthotopically, quail-derived tissue was found next to the anterior hindbrain and within the mandibular arch, in line with classical fate-mapping experiments (Couly et al., 1992; Noden, 1983a; Wachtler and Jacob, 1986) (n=4, Fig. 1B). The expression of lateral rectus EOM markers was confined to the territory adjacent to rhombomere 2, i.e. at the correct position (Mootoosamy and Dietrich, 2002). When the same tissue was grafted anteriorly next

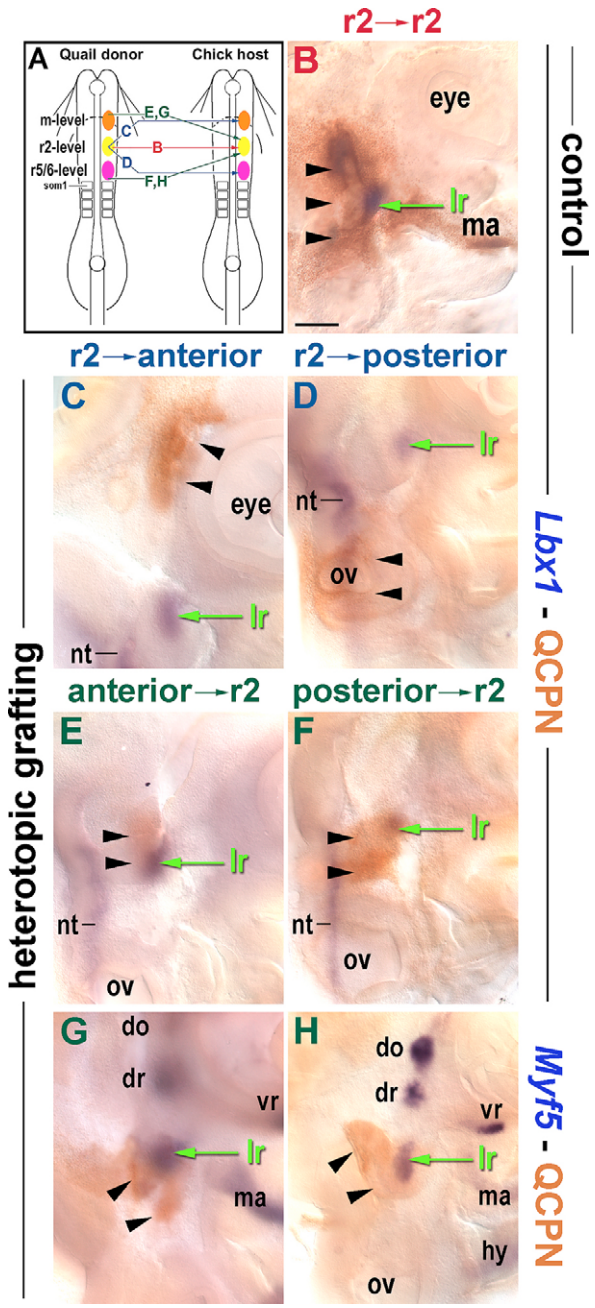

Fig. 1. Head mesoderm develops into muscle according to its local environment. (**A**) Scheme of operations at HH8-9⁻; dorsal view of embryos, anterior to the top. Quail-derived head mesoderm from rhombomere 2 levels was grafted orthotopically as control (**B**), anteriorly next to the anterior midbrain (**C**) or posteriorly next to otic levels/rhombomere 5-6 (**D**). In **E**,**G**, head mesoderm from midbrain levels was grafted next to rhombomere 2; in **F**,**H**, head mesoderm from otic levels/rhombomere 5-6 was grafted next to rhombomere 2. (B-H) Lateral view of the heads of operated embryos at HH19; anterior to the top, dorsal to the left, ventral (branchial arches) to the right. Quail tissues were detected with the QCPN antibody (brown), the lateral rectus EOM with *Lbx1* (B-F; blue; note: additional expression in the neural tube), and muscle anlagen in general with *Myf5* (G,H, blue). Note that the molecular markers showed normal expression patterns. Scale bar: 200 μm. do, dorsal oblique EOM; dr, dorsal rectus EOM; hy, hyoid arch; lr, lateral rectus EOM; m, midbrain; ma, mandibular arch; nt, neural tube; ov, otic vesicle; r, rhombomere; som, somite; vr, ventral rectus EOM.

to the anterior midbrain (*n*=4; Fig. 1C) or posteriorly to otic levels (*n*=2; Fig. 1D), the lateral rectus markers were not expressed in the graft. However, normal expression was seen at the usual site of the developing lateral rectus, next to rhombomere 2 (arrows). This was also the case when head mesoderm from anterior midbrain levels (*n*=6; Fig. 1E) or from otic levels (*n*=6; Fig. 1F) was heterotopically grafted to anterior hindbrain levels (arrows). The normal development of muscle anlagen upon the heterotopic grafting of anterior or posterior head mesoderm fragments to rhombomere 2 levels was confirmed by *Myf5* staining (Fig. 1G,H). Moreover, operated and unoperated sides of the embryos looked identical (not shown). This suggests that head muscles develop in

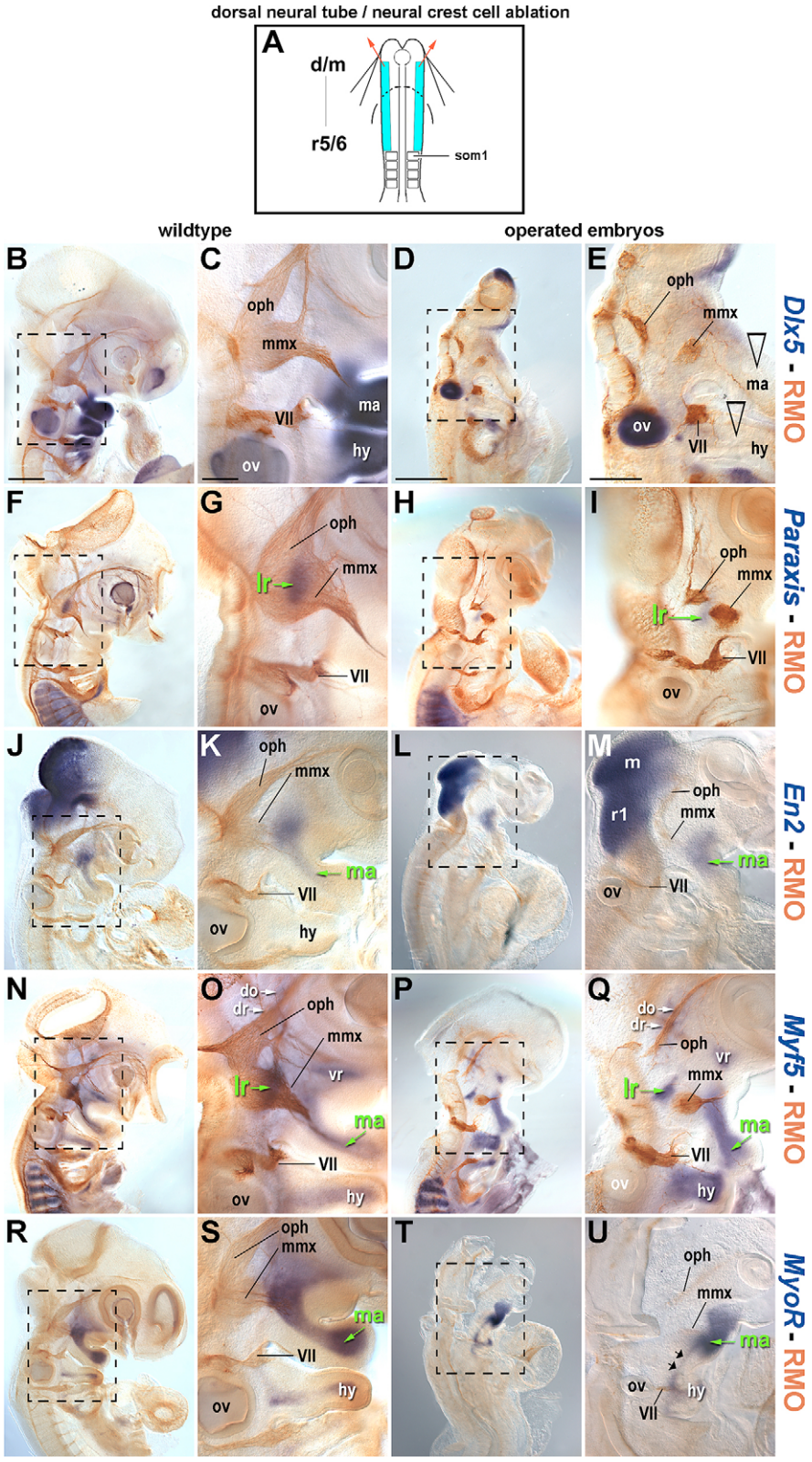

Fig. 2. Neural crest cells are dispensable for early head muscle differentiation and specification. (**A**) Scheme of dorsal neural tube/neural fold ablation at HH8 to remove neural crest cells. Dorsal view, anterior to the top, ablated area in turquoise. (**B**,**F**,**J**,**N**,**R**) Heads of unoperated embryos; (**C**,**G**,**K**,**O**,**S**) higher magnification of the lateral rectus/MAM region corresponding to boxed area in B,F,J,N,R. (**D**,**H**,**L**,**P**,**T**) Operated embryos (**E**,**I**,**M**,**Q**,**U**) higher magnification of lateral rectus/MAM region as indicated in D,H,L,P,T. Embryos are at HH19; lateral views, anterior is to the top, dorsal to the left. Embryos are double stained with the RM0270 antibody to trace the nervous system (brown). (B-E) *Dlx5* expression. (B,C) In wild-type embryos, *Dlx5* is predominantly expressed in the neural crest cells filling the branchial arches. (D,E) Operated embryo. While *Dlx5* expression in the derivatives of the nasal and otic placodes and expression in the maxillary and mandibular ectoderm remained, the neural-crest-associated expression is absent (open arrowheads). Moreover, the ophthalmic and the mandibulomaxillary aspect of the trigeminal ganglion are separate. This indicates that the surgical procedure was successful. (F-I) *Paraxis* expression. Both in the wild type (F,G) and in the operated embryo (H,I), *Paraxis* labels the developing lateral rectus EOM. (J-M) *En2* expression. *En2* is expressed in the mandibular arch muscles of both the unoperated (J,K) and the operated (L,M) embryo. (N-Q) *Myf5* expression. In the wild type (N,O), muscle anlagen for the mandibular and hyoid arch muscles and the lateral rectus, dorsal oblique, dorsal rectus and ventral retcus EOM are differentiating and express *Myf5*. This is also the case for neural crest ablated embryos (P,Q). (R-U) *MyoR* expression. *MyoR* expression associated with the ventral/branchiomeric muscle anlagen is present in the wild type (R,S) and operated (T,U) embryo. Note that in the absence of neural crest cells, the *MyoR* expression domains remained proximally unsegregated (small arrows). Scale bars: 400 μm in B,F,J,N,R; 200 μm in C,G,K,O,S; 400 μm in D,H,L,P,T; 200 μm in E,I,M,Q,U. d, diencephalon; do, dorsal oblique EOM; dr, dorsal rectus EOM; hy, hyoid arch; ma, mandibular arch; mmx, mandibulomaxillary aspect of the trigeminal; oph, ophthalmic aspect of the trigeminal (Vth) nerve; ov, otic vesicle; r, rhombomere; VII, facial nerve; vr, ventral rectus EOM.

tune with their local environment (ortsgemäss). This furthermore suggests that extrinsic cues govern the development of head muscles.

Ablation of neural crest cells

As neural crest cells have been implicated in head myogenesis (Noden, 1983b), they were the first candidates in our quest to identify signals positively regulating head muscle differentiation and specification. To investigate their role in vivo, the neural folds and the dorsal third of the neural plate were ablated bilaterally from diencephalic to otic levels at HH8-9^{-} (n=34), as indicated in Fig. 2A. This operation eliminates the source of neural crest cells and prevents crest regeneration (Begbie et al., 1999; Lumsden et al., 1991; Veitch et al., 1999). To confirm that this was the case, embryos at HH19 were analysed for the expression of *Dlx5*, a marker for branchial arch neural crest (Ferrari et al., 1995) (Fig. 2B-E). Indeed, operated embryos lacked neural-crest-associated *Dlx5* expression (Fig. 2D,E, open arrowheads). Moreover, tracing the nervous system with the RMO antibody, we found the typical neuronal phenotype of neural-crest-deficient embryos, namely a separation of the ophthalmic and the mandibulomaxillary aspect of the trigeminal ganglion (Begbie et al., 1999; Veitch et al., 1999) (Fig. 2D,E, oph, mmx). Next, we investigated the muscular phenotypes of the operated embryos, judging the neural-crest ablated state of the embryos on the basis of their neuronal phenotype. We found that the lateral rectus EOM markers were appropriately expressed at the level of rhombomere 2 (*Paraxis*: Fig. 2F-I, *Lbx1* not shown). Likewise, *En2* correctly labelled the MAM (Gardner and Barald, 1992) (Fig. 2J-M). The *Myf5* expression pattern indicated that in the absence of neural crest cells, the head mesoderm occupied all the available space in the branchial arches. Importantly, all differentiating muscle anlagen present in the wild type were also present in the operated embryos (Fig. 2N-Q). Finally, *MyoR*, a marker for proliferative, undifferentiated arch muscle precursors (von Scheven et al., 2006) was present, although expression domains remained proximally unsegregated (Fig. 2R-U, small arrows). Thus, neural crest cells seem to play a role in the spacing and separation of muscle anlagen, but not in the initiation of muscle differentiation or EOM-MAM specification.

Ablation of the eye

The eye is the target of the developing EOM, and in *ZRDCT-An* anophthalmic mouse mutants lacking eyes, EOM are strongly reduced (Paterson and Kaiserman-Abramof, 1981). To investigate whether the eye is responsible for EOM differentiation and specification, at HH10 we unilaterally ablated the optic placode and the part of the forebrain providing the optic cup (Fig. 3A; n=11). After reincubation for 48 hours, the embryos were assayed for the expression of the lateral rectus markers and, using a *Myf5* probe, for the presence of head muscles in general. The ablation was controlled using the *Pax6* antibody (Fig. 3B-E, brown colouring). Upon staining, the embryos were bisected mid-sagittally, and both halves were photographed and compared. We found that on the operated side only a small remnant of the optic stalk was present, while the eye was lacking (Fig. 3C,E, open arrowheads). Significantly, *Paraxis* (not shown), *Lbx1* (Fig. 3C, blue staining) and *Myf5* (Fig. 3E, blue staining) were correctly expressed. Thus, early muscle differentiation and specification does not rely on the presence of the muscles' target.

Prevention of lateral rectus eye muscle innervation

EOM formation has been suggested to depend on the presence of the cognate nerves (Engle, 2002). To test this hypothesis, lateral rectus innervation was prohibited by surgically removing rhombomeres 5 and 6 at HH10 (n=10; Fig. 4B). At HH19-20, the nervous system was traced with the RMO antibody (brown staining), and the lateral rectus EOM using a probe for *Lbx1* (not shown) or *Paraxis* (blue staining). The embryos were then mid-sagittally bisected and viewed from the inside. On the unoperated side, the rootlets of the abducens

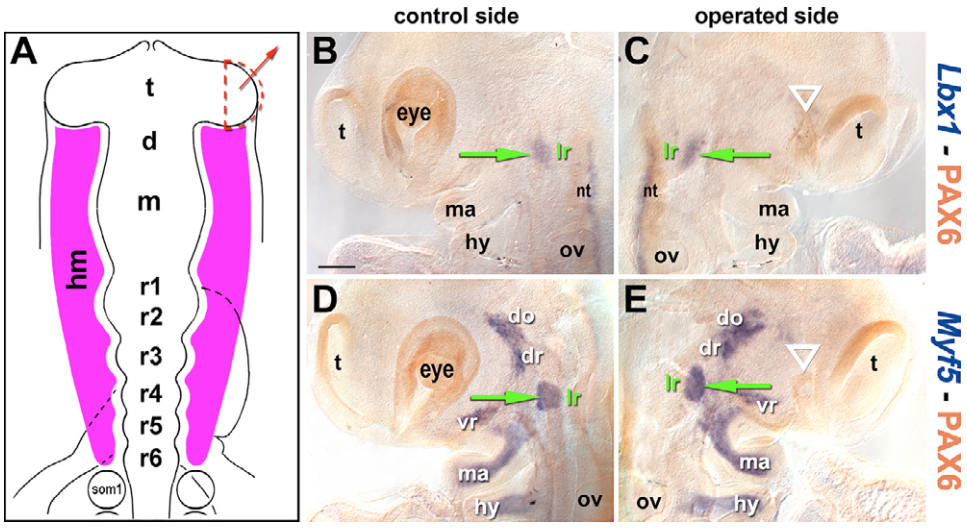

Fig. 3. The presence of the eye is not required for eye muscle differentiation and specification. (**A**) Scheme of eye ablation at HH10; dorsal view, anterior to the top. The optic placode and the region of the forebrain delivering the optic cup were removed. Pink: unsegmented head mesoderm. (**B-E**) Lateral views of HH19 heads; anterior to the top, dorsal to the right for unoperated sides (B,D), dorsal to the left for operated sides (C,E). (B-E) Brown staining: Pax6 antibody staining detecting strong expression in the telencephalon (t), eye, neural tube (nt)/hindbrain. Note, in operated embryos the eye is missing; only the rest of the optic stalk remained (C,E, open arrowhead). (B,C) *Lbx1* (blue staining) revealing normal lateral rectus anlagen. (D,E) Also *Myf5* expression (blue) is wild type. Scale bar: 200 μm. do, dorsal oblique EOM; dr, dorsal rectus EOM; hm, unsegmented head mesoderm; hy, hyoid arch; lr, lateral rectus EOM; ma, mandibular arch; nt, neural tube; ov, otic vesicle; t, telencephalon; vr, ventral rectus EOM.

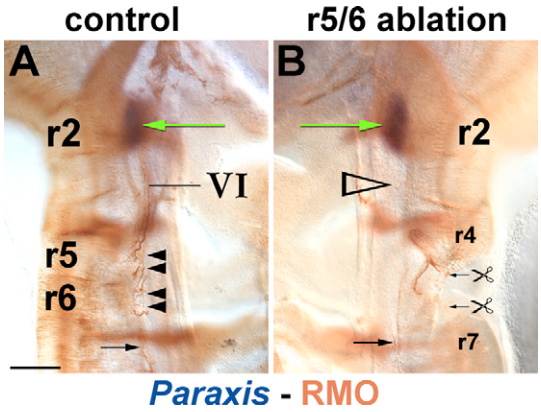

Fig. 4. Innervation does not control eye muscle differentiation and specification. Internal views of HH20 bisected chick heads; anterior to the top, dorsal to the left in **A** and right in **B**. Embryo stained for *Paraxis* expression (blue); nervous system traced with RMO270 in brown. (A) Unoperated control side. Note the abducens nerve (cranial nerve VI) with nerve rootlets in rhombomeres 5 and 6 (arrowheads) and axons having entered the *Paraxis* domain (arrow). (B) Rhombomeres 5/6 ablated side. The abducens nerve is missing (open arrowhead), but *Paraxis* is expressed normally. Scale bar: 200 μm. r, rhombomere; VI, abducens nerve.

nerve were clearly visible in the ventral region of rhombomeres 5 and 6 (Fig. 4A, arrowheads), with axons extending anteriorly, innervating the lateral rectus anlage (arrow) (Wahl et al., 1994). On the operated side, the abducens nerve was missing. However, *Paraxis* expression was identical to the unoperated side, indicating that for the onset of muscle development the nerve was dispensable.

Separation of the eye-muscle-delivering head mesoderm from surrounding tissues

Our study showed that extrinsic cues are required for early head muscle differentiation and specification. However, these cues are not, or not exclusively, provided by neural crest cells, target organ or cognate nerve. This suggests that tissues in the immediate vicinity of the muscle anlagen may account for their development. We therefore systematically investigated the roles of the neighbouring tissues. Six types of operations were carried out at HH10: (1) separation of neural tube and head mesoderm by inserting an impermeable barrier of tantalum foil at the level of rhombomere 2 (n=59); (2) separation of notochord and floor plate from the head mesoderm with foil introduced through the roof plate, then inserted lateral to floor plate/notochord (n=23); (3) separation of head mesoderm and surface ectoderm, making a cut at the neural tube-ectoderm interface, peeling the ectoderm back aided by dispase, then inserting foil underneath (n=19) (this operation also prevents contact with the trigeminal ganglion); (4) separation from the laterally located tissues in the mandibular arch by inserting foil laterally (n=18); (5) separation from anterior tissues by inserting foil perpendicular to the longitudinal body axis at the level of rhombomere 1 (n=6); (6) separation from posterior tissues by inserting foil perpendicular to the longitudinal body axis at the level of rhombomere 3 (n=8).

The embryos were analysed 48 hours after the operation for the expression of lateral rectus EOM markers, for MAM markers and for muscle differentiation markers. Moreover, the nervous system was traced with the RMO antibody except in the case of notochord/floor plate separation experiments, in which the notochord and floor plate were stained for the expression of *Shh*. To examine marker gene expression in detail, transverse vibratome sectioning at the level of rhombomere 2 and the mandibular arch was performed. However, only the experiments separating neural tube and head mesoderm led to significant changes in gene expression of the markers and are shown here (Fig. 5).

Separation of head mesoderm and neural tube-marker gene expression

When neural tube and head mesoderm were separated at HH10, as shown in Fig. 5A, Ai, then 48 hours later, the lateral rectus EOM was well established on the control side, expressing *Lbx1* (Fig. 5B,D, arrows) and *Paraxis* (Fig. 5E,G, arrows). On the operated side however, both markers were strongly reduced or absent (Fig. 5C,D,F,G, open arrowheads). This loss of EOM-marker expression was not due to the loss of the muscle anlage, as *Myf5* was expressed on the unoperated, as well as the operated, side (Fig. 5H-J, arrows). Likewise, the balance between muscle proliferation and differentiation was normal, as evidenced by the wild-type expression of *MyoR* (Fig. 5K-M, arrows). Thus, muscle differentiation commenced correctly, but the specification as lateral rectus EOM had failed.

To investigate whether the muscle in the position normally occupied by the lateral rectus may have adopted the fate of the laterally adjacent MAM, we stained the embryos for *En2* expression. On the unoperated side, *En2* signals were confined to the prospective jaw closure muscles developing in the mandibular arch, staying clear of the more medially located anlage of the lateral rectus EOM (Fig. 5N, arrows). On the operated side however, *En2* staining encompassed this muscle anlage (Fig. 5O,P, arrowheads). Thus, in absence of the neural tube derived signal, muscle in the position of the lateral rectus anlage differentiates, but lacks the lateral rectus markers and, instead, expresses markers for the mandibular arch muscles.

Separation of head mesoderm and neural tube-innervation phenotype

The specification of abducens motoneurons depends on positional information and patterning cues within rhombomeres 5 and 6 (Hernandez et al., 2004; Moens et al., 1998). However, the axons have to sample their environment to extend along the ventral surface of the neural tube in an anterior direction and to identify the lateral rectus muscle anlage, disregarding the laterally adjacent MAM and the more anteriorly located remaining five EOM (Wahl et al., 1994). It thus seems conceivable that lateral rectus specification and the target recognition of the abducens nerve are linked. We therefore blocked the neural tube derived signal for the lateral rectus muscle as before, cultivated the embryos to HH19-20, double stained for *Paraxis*-RMO and mid-sagittally opened the embryos to reveal the innervation patterns on the unoperated (Fig. 6A) and operated sides (Fig. 6B,C; n=17). We found that on the left, unoperated side, the *Paraxis*-expressing muscle anlage (arrowhead) was innervated by the abducens nerve (arrow). On the right, operated side that lacked *Paraxis*, the nerve showed a defasciculated appearance typical for axons not readily finding a target (Tosney and Landmesser, 1985) (arrowhead). This suggests that the communication between the re-specified lateral rectus anlage and the abducens nerve was defective.

Properties of the signal specifying the lateral rectus EOM

Transmission of the neural tube derived signal

The lateral rectus eye muscle anlage resides in close proximity to the neural tube before becoming engaged with the developing eye. Thus, its specification may be achieved either via a soluble signal or

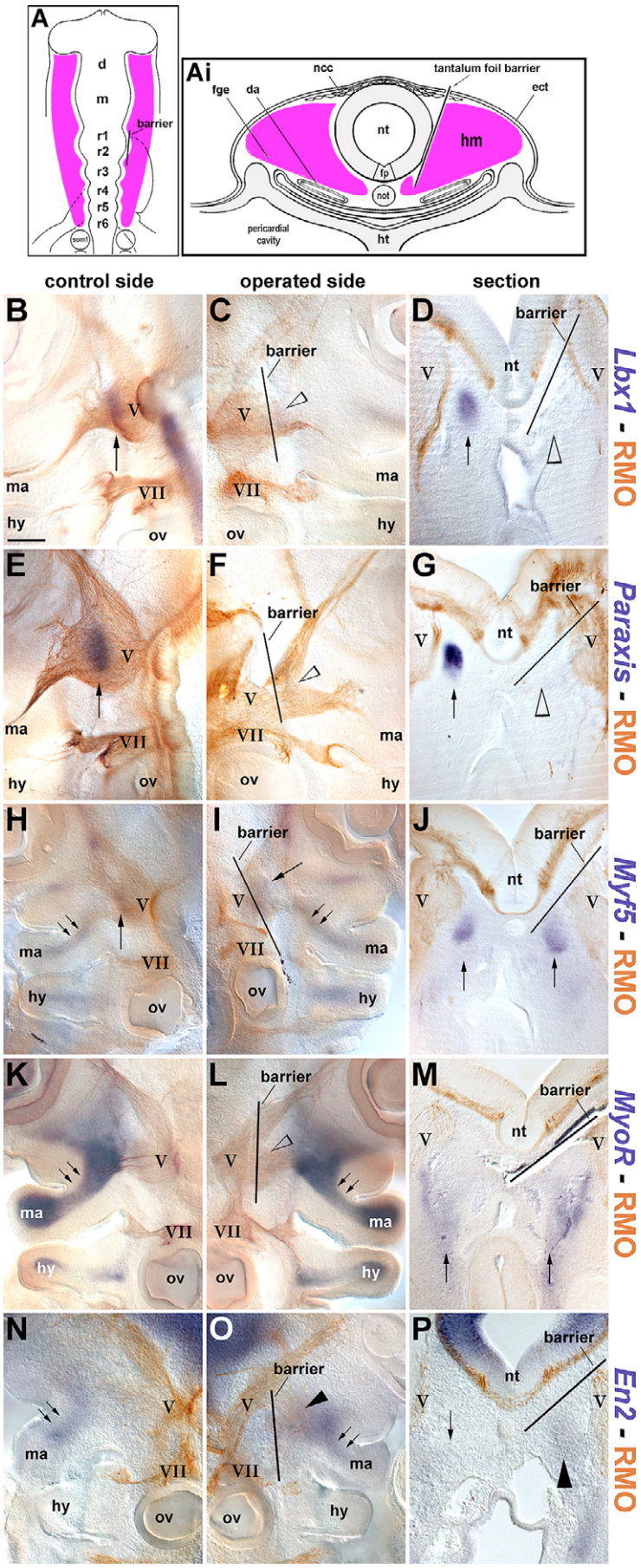

Fig. 5. The neural tube specifies the lateral rectus eye muscle. (**A**) Schematic dorsal view and (Ai) cross section (dorsal to the top) illustrating the surgical procedures at HH10; head mesoderm in pink, the position of the impermeable barrier (tantalum foil) is indicated. (**B**,**E**,**H**,**K**,**N**) Lateral views of unoperated sides; anterior to the top, dorsal to the right. (**C**,**F**,**I**,**L**,**O**) Lateral views of operated sides; anterior to the top, dorsal to the left. (**D**,**G**,**J**,**M**,**P**) Cross sections at anterior hindbrain/mandibular arch levels; dorsal to the top, operated sides to the right, markers and the position of the barriers are indicated. Note that upon separation of the neural tube from the head mesoderm, the lateral rectus markers *Lbx1* (B-D) and *Paraxis* (E-G) failed to be expressed. *Myf5* (H-J) and *MyoR* (K-M) expression continued. *En2* expression (N-P) spread form the mandibular arch muscle anlage medially, encompassing the muscle normally expressing the lateral rectus markers. Thus, muscle specification, but not differentiation, was perturbed. Scale bar: 200 μm. d, diencephalon; da, dorsal aorta; ect, surface ectoderm; fge, foregut endoderm; fp, floor plate of the neural tube; ht, heart; hy, hyoid arch; m, midbrain; ma, mandibular arch; ncc, neural crest cells; not, notochord; nt, neural tube; ov, otic vesicle; r, rhombomere; V, trigeminal ganglion; VII, facial nerve.

through cell-cell contact. To investigate this, we used the same strategy as for the earlier barrier experiments; this time, however, inserting a 25-mm-thick filter with a pore size of 0.05 μm between the anterior hindbrain and the head mesoderm. This filter excludes cellular extensions but admits soluble factors (Fan and Tessier-Lavigne, 1994) (*n*=16, Fig. 6D-F). The embryos were analysed for the expression of *Paraxis* and double stained with the RMO antibody for their innervation phenotype. Notably, on the operated side, both *Paraxis* expression and innervation of the lateral rectus by the abducens nerve was restored (Fig. 6E,F, arrows).

Spatial restriction of the neural tube derived signal

Rhombomeres of the hindbrain each carry a distinct identity (Irving and Mason, 2000). With the lateral rectus EOM developing next to rhombomere 2, we asked whether the neural-tube-derived signal required for the development of this muscle would be rhombomere 2-specific. For this, two sets of experiments were carried out: (1) heterotopic grafting of neural tissues (Fig. 7); and (2) transformation of rhombomere 2 via *Hoxb1* misexpression (Fig. 8).

Heterotopic neural tube grafting

Rhombomeres, when grafted to a posterior position, lose their positional values unless the isthmus is included (Irving and Mason, 2000). Therefore, we transplanted at HH10 rhombomere 2 orthotopically as control (Fig. 7B, *n*=3), but heterotopically grafted rhombomere 2 plus the anteriorly adjacent r1, isthmus and posterior midbrain to anterior midbrain-diencephalic levels (Fig. 7C, *n*=3) or otic levels (Fig. 7D, *n*=5), and we grafted the posterior diencephalon-anterior mesencephalon (Fig. 7E, *n*=4) or the posterior hindbrain (Fig. 7F, *n*=7) to midbrain-rhombomere 2 levels. The scheme of transplantations is shown in Fig. 7A. In all cases, the lateral rectus marker *Lbx1* was expressed at the normal site, indicating that the neural tube derived signal is not rhombomere 2-specific, and furthermore, not sufficient to trigger lateral rectus EOM development at an ectopic location.

Hoxb1 misexpression

Hoxb1 controls the identity of rhombomere 4 and, when misexpressed in rhombomere 2, homeotically transforms rhombomere 2 into rhombomere 4 (Bell et al., 1999). We electroporated at HH10 either the pCAβ-IRES-eGPF control vector (Alvares et al., 2003); (Fig. 8B-D, *n*=5) or this vector expressing mouse *Hoxb1* (Fig. 8E-G, *n*=11) into the posterior midbrain-anterior hindbrain, using the conditions established by Schubert and Lumsden (Schubert and Lumsden, 2005) (shown schematically in Fig. 8A). However, neither the lateral rectus EOM marker *Paraxis* (Fig. 8C,F) nor the muscle marker *Myf5* (Fig. 8D,G) were affected. Thus, consistent with our heterotopic grafting experiments, the signal supporting lateral rectus EOM development is not confined to rhombomere 2.

Test for neural tube derived signalling molecules

Our analysis suggested that a soluble, anteroposteriorly unrestricted signal from the neural tube acts in lateral rectus EOM specification. Shh derived from the floor plate and Wnt1 derived from the dorsal neural tube fit this description (Brent and Tabin, 2002). We therefore inserted beads loaded with 100 μg/ml recombinant Shh protein (*n*=6) or RatB1 cells engineered to release Wnt1 (Cheng et al., 2004; Fan et al., 1997; Münsterberg et al., 1995) (*n*=13) into the head mesoderm at the level of the future lateral rectus EOM (Fig. 9A). As controls, beads loaded with bovine serum albumin (BSA) (*n*=12) and RatB1 fibroblast carrying the empty cloning vector (*n*=2) were used. We expected to find an upregulation of the lateral rectus markers in response to Shh or Wnt1. Instead, Wnt1 slightly, Shh strongly suppressed *Paraxis* (see Fig. S1 in the supplementary material), in line with their repressive function for head myogenesis described in (Tzahor et al., 2003).

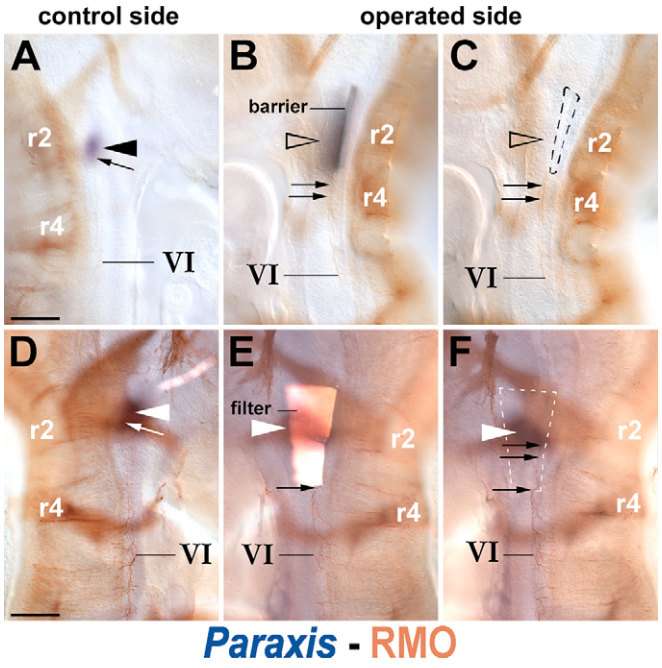

Fig. 6. The signal from the neural tube is a soluble factor. Internal views of *Paraxis*-RMO270 stained, bisected embryo at HH20. (**A**,**D**) Unoperated control sides, (**B**,**C**,**E**,**F**) operated sides before (B,E) and after (C,F) removal of the barrier or filter. Anterior is to the top, dorsal to the left in A,D; to the right in B,C,E,F. Position of the barrier or filter is indicated. (A-C) Separation of neural tube and head mesoderm with tantalum foil, an impermeable barrier. Note that on the control side the abducens nerve is well fasciculated and innervated the *Paraxis*-expressing lateral rectus anlage (A). On the operated side (B,C), the nerve is defasciculated and did not reach the area that normally would express *Paraxis* next to rhombomere 2. (D,E) Separation of neural tube and head mesoderm with a polycarbonate filter that admits soluble factors. Note that *Paraxis* is expressed on the operated side. Moreover, the abducens nerve navigated around the filter and innervated the *Paraxis*-expressing lateral rectus. Scale bar: 200 μm. r, rhombomere; VI, abducens nerve.

Signals for the branchial arch muscles

Our experiments indicated that the signal from the neural tube simultaneously specifies the lateral rectus EOM and suppresses markers for the neighbouring MAM. We thus asked whether signals from the branchial arches might suppress EOM and support MAM development. As ablation experiments in this area are not feasible because they disturb arch patterning as a whole, injure the aortic arches and lead to fatal bleeding, we performed candidate gene/gain-of-function experiments.

Signalling molecules known to influence branchial arch development are Fgf and Bmp molecules (Helms et al., 2005). Importantly, receptors for these molecules are expressed in the head mesoderm and developing muscles (S.D., unpublished). Moreover, Fgf and Bmp molecules are expressed in the pharyngeal endoderm at HH10, the time *MyoR* expression commences (von Scheven et al., 2006) (Fig. 9Ai,iii). Subsequently, elevated signals are found in the pharyngeal pouches (endoderm plus ectoderm) and the oral

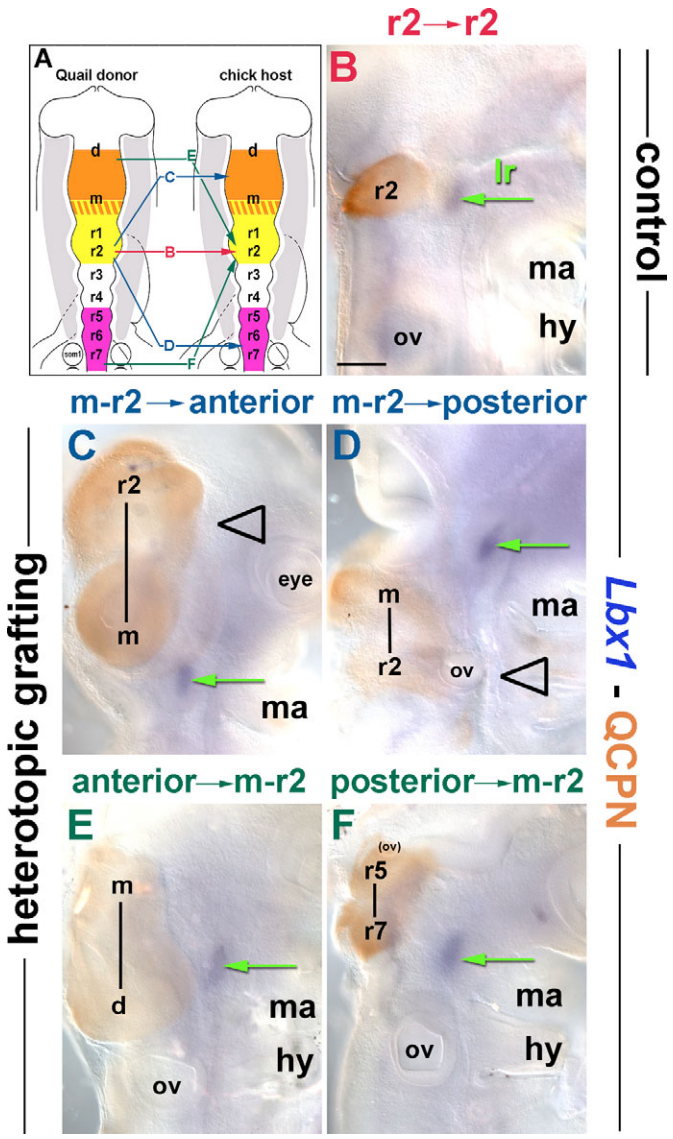

Fig. 7. The signal from the neural tube is not sufficient to trigger lateral rectus development. (**A**) Scheme of quail-chick neural tube grafting at HH10; dorsal view, anterior to the top. (**B-F**) Lateral views of operated embryos at HH19, stained for the lateral rectus marker *Lbx1* in blue and the quail cell marker QCPN in brown; anterior to the top, dorsal to the left. The anteroposterior orientation of the grafts is indicated. (B) Orthotopic control grafting of rhombomere2; *Lbx1* is expressed at the normal location (green arrow). (C) When the neural tube from posterior midbrain to rhombomere 2 levels was grafted in place of midbrain and posterior diencephalon, the ectopic rhombomere 2 did not trigger ectopic *Lbx1* expression (open arrowhead). (D) Similarly, no ectopic *Lbx1* expression occurred when the graft was transplanted in place of rhombomeres 4-6 (open arrowhead). (E) When the posterior midbrain to rhombomere 2 was replaced with neural tissues from anterior midbrain to diencephalic levels, *Lbx1* was expressed at the normal location dorsal to the mandibular arch (green arrow). (F) Grafting of the posterior hindbrain, including parts of the otic placode to midbrain-rhombomere 2 levels, led to the development of an ectopic otic vesicle, and also permitted *Lbx1* expression (green arrow). Scale bar: 200 μm. d, diencephalon; hy, hyoid arch; lr, lateral rectus EOM; m, midbrain; ma, mandibular arch; ov, otic vesicle; r, rhombomere.

ectoderm (shown for HH19, Fig. 9ii,iv). Thus, recombinant Fgf4, Fgf8, Bmp2, Bmp4 or Bmp7 protein was loaded onto beads at 500 μg/ml or 100 μg/ml. Subsequently, the beads were implanted into the head mesoderm at the level of rhombomere 2 (Fig. 9A). As a control, BSA-soaked beads were used (Fig. 9B-E). Beads loaded with Fgf molecules gave identical results; here only the Fgf8 experiments at 100 μg/ml are shown (n=30, Fig. 9F-O). Also all Bmp molecules led to the same phenotypes. However, at 500 μg/ml, we observed strong bilateral effects. Thus, we focus here on the phenotype obtained with Bmp7 at 100 μg/ml, which left the control side intact (n=18, Fig. 9P-W).

Effect of Fgf8

Fgf8 beads, when implanted into the neural tube, mimic the function on the isthmic organiser, suppress *Hoxa2* and anteroposteriorly re-pattern the hindbrain (Irving and Mason, 2000). Although our heterotopic neural tube grafting and *Hoxb1* misexpression experiments deemed this unlikely, we tested whether Fgf8 beads implanted into the head mesoderm might also re-pattern the neural tube, thereby indirectly influencing muscle development. However, the operation did not affect positional values in the neural tube, as monitored by *Hoxa2* expression (Fig. 9F,G, n=7). Yet Fgf8 had a strong effect on the craniofacial muscle markers (Fig. 9H-O, n=39). The molecule downregulated the expression of lateral rectus EOM markers (shown for *Paraxis*, Fig. 9H,I, open arrowhead) and upregulated the expression of the MAM marker *En2* (Fig. 9L,M, arrowhead), thus evoking a phenotype similar to that obtained by the neural tube-head mesoderm separation experiments. Unlike those, however, *Myf5* expression was downregulated (Fig. 9J,K, open arrowhead), while *MyoR* was upregulated (Fig. 9N,O, arrowhead). Thus, Fgf8 supported the MAM over the EOM fate, but at the same time kept the cells specified as MAM in an immature, proliferative state.

The isthmus is a prominent source of Fgf8, but in the neighbouring EOM, neither *En2* nor *MyoR* expression are found. We therefore tested the ability of the isthmus to signal to adjacent mesoderm, employing limb induction from the flank lateral mesoderm as a well-established Fgf8 response assay (Cohn et al., 1995). Fgf8-loaded beads (n=3) or HH10 posterior midbrain-anterior hindbrain (n=6) were implanted at HH16 as described by Lours and Dietrich (Lours and Dietrich, 2005). Forty-eight hours later, we found that the Fgf8 beads had induced ectopic limbs carrying *Fgf8*-expressing apical ectodermal ridges, while the isthmus, though maintaining its own *Fgf8* expression, had not (see Fig. S2 in the supplementary material).

Effect of Bmp7

Bmp7 beads (Fig. 9P-W, n=23) downregulated the lateral rectus markers (shown for *Paraxis*, Fig. 9P,Q, open arrowhead), but also reduced *En2* expression in the distal area of the mandibular arch (Fig. 9T,U, open arrowheads). Moreover, *Myf5* expression was eliminated, both in the area of the lateral rectus and in the mandibular arch (Fig. 9R,S, arrowheads). *MyoR* expression was slightly downregulated (Fig. 9T,U, open arrowheads). Thus, Bmp7 has a generalised effect on the developing head muscles, halting their progress of differentiation.

DISCUSSION

Head muscles fulfil versatile yet vital functions in the body (Goodrich, 1958). Despite their importance, their development is still a mystery. In this study, we aimed at shedding light onto the control of early muscle differentiation and specification of head

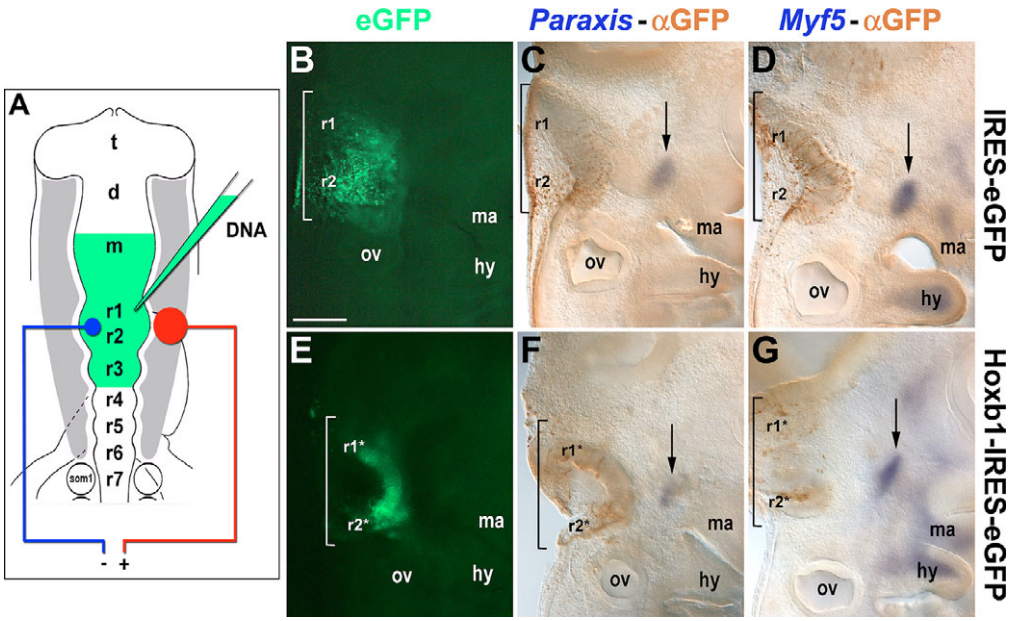

Fig. 8. The signal from the neural tube is not rhombomere 2-specific. (**A**) Scheme of neural tube electroporation at HH10. (**B-G**) Lateral views of electroporated embryos at HH19; anterior to the top, dorsal to the left. (B,E) The targeted area revealed by means of eGFP fluorescence. (C,D,F,G) *Paraxis* (C,F) or *Myf5* (D,G) expression in blue and staining with the anti-GFP antibody in brown. Same embryo shown in B,C and E,F, respectively. (B-D) Control electroporation with the pCAβ-IRES-eGFP vector lacking the open reading frame for *Hoxb1* allows normal expression of *Paraxis* and *Myf5*. (E-G) Misexpression of *Hoxb1* in the anterior hindbrain transforms the identity of rhombomeres into that of rhombomere 4 (r1*, r2*). However, *Paraxis* and *Myf5* expression are not perturbed. Scale bar: 250 μm. d, diencephalon; hy, hyoid arch; m, midbrain; ma, mandibular arch; ov, otic vesicle; r, rhombomere; t, telencephalon.

muscles derived from the non-somitic head mesoderm. We focused on the region of the anterior hindbrain, because here eye muscles forming outside the arches and jaw closure muscles developing within the mandibular arch reside side by side. Moreover, besides Myf5, a muscle-determining factor indicating the onset of muscle differentiation (Noden et al., 1999), these muscles differentially express a set of markers with *Lbx1* and *Paraxis* labelling the lateral rectus EOM (Mootoosamy and Dietrich, 2002), *En2* labelling the MAM (Gardner and Barald, 1992) and *MyoR* labelling the proliferative, undifferentiated MAM precursors (von Scheven et al., 2006). Thus, we are in the fortunate position of being able to simultaneously investigate muscle differentiation and specification.

Our study shows that head muscle development is controlled by extrinsic cues. Yet tissues long suspected to control head myogenesis – namely neural crest cells, target organ and innervating nerve – are dispensable for early muscle differentiation and specification. However, we identified a signal from the neural tube that positively regulates the expression of the EOM markers and negatively regulates the MAM markers. This signal is soluble and, together with a further factor, specifies the lateral rectus EOM, possibly to aid its innervation. Furthermore, we identified arch-based Fgf8 as a positive regulator for MAM and negative regulator of EOM specification, thus serving as antagonist to the neural tube derived signal. However, Fgf8 had an additional function in regulating muscle differentiation, which was distinct from the effect of Bmp7 (data summarised in Table 1).

Head muscle development depends on signals from the local environment

We recently showed that the head mesoderm is predisposed to follow a specific head programme of myogenesis (Mootoosamy and Dietrich, 2002). Moreover, the various head muscles develop at defined, stereotype positions, and eventually, the lateral rectus EOM and the MAM express distinct markers (Couly et al., 1992; Gardner and Barald, 1992; Mootoosamy and Dietrich, 2002; Noden, 1983a; Wachtler and Jacob, 1986). In addition, the head mesoderm possesses positional information, which it can superimpose onto stray neural crest cells (Trainor and Krumlauf, 2000). Thus, it was equally possible that head myogenesis is controlled by intrinsic or extrinsic cues. Grafting fragments of head mesoderm into heterotopic locations showed, however, that head muscle differentiation and specification is controlled by signals from the local environment. Head mesoderm from midbrain or otic levels grafted to the level of the anterior hindbrain initiated myogenesis and expressed the lateral rectus markers in the same fashion as the endogenous muscle anlage on the control side. Conversely, when head mesoderm normally providing this muscle was moved to the anterior midbrain or to otic levels, then muscle development proceeded in accordance with the new position and the lateral rectus markers were not expressed. Thus, while the head mesoderm is bound to employ a myogenic programme distinct from myogenic programmes in the trunk, the onset of this programme and the specification of individual muscles rely on instructive cues from the environment.

Neural crest cells, target tissues and nerves are dispensable for early head muscle development

Classically, head myogenesis was thought to depend on neural crest cells (Grammatopoulos et al., 2000; Noden, 1983b; Pasqualetti et al., 2000), target tissues (Paterson and Kaiserman-Abramof, 1981) and innervating nerves (Engle, 2002). However, when the head mesoderm was separated from these tissues through ablation experiments then muscle differentiation and specification commenced correctly. Thus, neural crest cells, target tissues and

Table 1. Summary of manipulations affecting head muscle specification and differentiation

	Markers for			
	Muscle pattern		Muscle differentiation	
Treatment	Lateral rectus extraocular muscle: *Paraxis*, *Lbx1*	Mandibular arch muscles: *En2*	Differentiating muscle precursors: *Myf5*	Proliferative, undifferentiated muscle precursors (branchial arches): *MyoR*
Separation neural tube – head mesoderm	Downregulation	Upregulation	Normal	Normal
Fgf8 beads	Downregulation	Upregulation	Downregulation	Upregulation
Bmp7 beads	Downregulation	Proximal: normal Distal: downregulation	Downregulation	Mild downregulation

Signal from neural tube: specifies lateral rectus EOM, suppresses mandibular arch muscle identity; no effect on the progress of differentiation. Fgf8: dual function (1) suppression of lateral rectus and support of mandibular arch muscle identity, (2) support of muscle precursor proliferation over differentiation. Bmp7: suppression of skeletal muscle development.

innervating nerves are not necessary for early head muscle development in vivo. Our findings contrast with recent in-vitro experiments showing that cranial neural crest cells promote head muscle differentiation (Tzahor et al., 2003). It has to be noted, however, that in the trunk, somitic myogenesis is controlled by various surrounding tissues, of which the dorsal neural tube and the surface ectoderm show a degree of redundancy (Dietrich et al., 1997). If signal redundancy also occurs in the head, then the in-vivo role of the neural crest cells may become masked by other tissues fulfilling a similar function. However, in vitro the head mesoderm expressed a number of cardiac markers (Tzahor et al., 2003). Thus, it is possible that under the chosen culture conditions, the neural crest cells were required to override the signals recruiting mesoderm for cardiac development.

As our work suggests that neural crest cells and innervation are dispensable for early head muscle development, this implies that the reported role of neural crests cells and nerves affects head muscle development after the onset of differentiation and specification. Remarkably, studies on somitic myogenesis established that in the trunk, muscle, connective tissues and nerves begin their development independently. However, after the completion of this initial phase, these tissues become interdependent (Hippenmeyer et al., 2004; Kardon, 1998; Pun et al., 2002). Thus, it is possible that although the onset of myogenesis in head and trunk is controlled by distinct programmes, eventually these programmes may converge. In the trunk, connective tissue is mesoderm-derived, while in the head it stems from neural crest cells (Couly et al., 1993; Noden, 1983a). Moreover, in the trunk skeletal muscle is innervated by somatic motoneurons, while in the head, the branchial arch muscles are supplied by neurons resembling visceral motoneurons (Jacob et al., 2001). It thus will be crucial to investigate whether the distinct tissues serving the similar functions employ related or different molecular cascades.

A soluble signal from the neural tube specifies the lateral rectus versus mandibular arch muscles

Searching for the extrinsic cues that might control the early events in head muscle formation, we found that most tissues had no effect (or the effect was masked through signal redundancy). However, the neural tube provided a signal that promoted the expression of the lateral rectus EOM markers. In the absence of the neural tube derived signal, while all muscle anlagen differentiated at the appropriate position, *Paraxis* and *Lbx1* expression was lost. Instead, the muscle anlage normally providing the lateral rectus expressed *En2*, a marker for MAM (Gardner and Barald, 1992). This suggests that the neural tube specifies the lateral rectus eye muscle versus the MAM.

Given the proximity of the neural tube to the lateral rectus, it was conceivable that the neural tube might transmit its signal through cell-cell contact. However, when a filter with a pore size of 0.05 μm was inserted between neural tube and head mesoderm, thereby preventing cell-cell contact but admitting soluble molecules (Fan and Tessier-Lavigne, 1994), then the expression of the lateral rectus markers was restored. This suggests that the neural tube releases a soluble factor.

To make inroads into the identification of the neural tube derived signal, we performed heterotopic grafting of neural tissues and changed the identity of the neural tube next to the lateral rectus EOM. These experiments showed that the neural tube derived signal is not sufficient to trigger ectopic lateral rectus development. Moreover, the signal is not confined to rhombomere 2, which neighbours the lateral rectus. This suggests that the neural-tube-derived signal might act in a permissive, rather than instructive, fashion.

Shh provided by the floor plate and Wnt1 by the dorsal neural tube are soluble signalling molecules that operate at all axial levels (Brent and Tabin, 2002); they hence fit the phenomenological description of the elusive neural tube derived signal. However, in gain-of-function experiments, these molecules, instead of promoting the expression of the lateral rectus markers, suppressed them. This observation is in line with our earlier collaborative study showing a repressive role for Shh and Wnt signals in craniofacial myogenesis (Tzahor et al., 2003).

Branchial-arch-based Fgf8 antagonises the neural tube signal and specifies MAM

It is established that during trunk muscle development, signals from the neural tube and lateral mesoderm act antagonistically to specify epaxial and hypaxial muscle precursors (Parkyn et al., 2002). As in the absence of the neural tube, MAM markers were ectopically expressed, we asked whether signals from the branchial arches might specify MAM but suppress EOM development.

Fgf8 and Bmp7 are known regulators of branchial arch pattern and development; they are expressed in the pharyngeal endoderm, pharyngeal pouches (endo- and ectoderm) and oral ectoderm and act in epithelial-mesenchymal interactions (Helms et al., 2005). Performing gain-of-function experiments, we found that Fgf8, but not Bmp7, had a specific effect on EOM and MAM markers. When Fgf8 beads were implanted into the mesoderm destined to form the lateral rectus, the EOM markers were lost and *En2* was ectopically expressed. This effect was not an indirect consequence of neural tube re-patterning, as *Hoxa2* expression was unaltered. The head mesoderm harbours Fgf receptors (S.D., unpublished), and in Fgf8

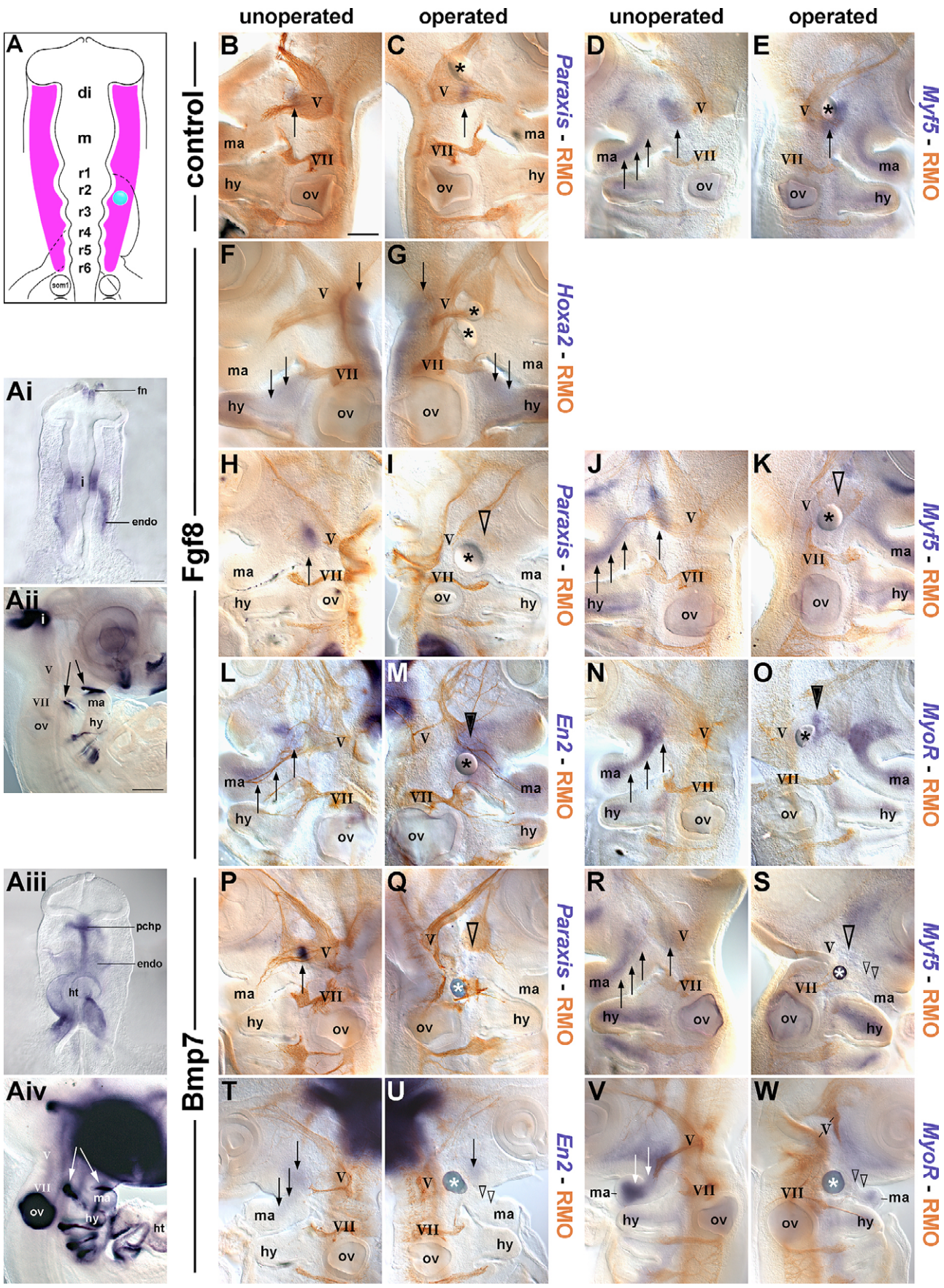

Fig. 9. See next page for legend.

Fig. 9. Differential effect of the mandibular-arch-derived signals Fgf8 and Bmp7. (**A**) Scheme of bead implantation at HH10, orientation as in Fig. 3A. (Ai,ii) *Fgf8* expression at HH10 (Ai, dorsal view, anterior to the top) and HH19 (Aii, lateral view of right side, anterior to the top). Note persistent expression of *Fgf8* in the pharyngeal endoderm and at HH19, upregulated expression in the oral ectoderm and in the endoderm plus overlying ectoderm of each pharyngeal pouch (Aii, arrows point towards expression associated with the mandibular arch). (Aii,iv) *Bmp7* expression at HH10 (Ai, ventral view, anterior to the top) and HH19 (Aii, lateral view of right side, anterior to the top). Note the persistent expression of *Bmp7* in the HH10 endoderm and heart; at HH19 expression is upregulated in the pharyngeal pouches, the oral ectoderm (arrows), and the in- and outflow tract of the heart. *Fgf8* and *Bmp7* are absent from the area of the lateral rectus EOM underneath the trigeminal ganglion. (**B-E**) Lateral views of embryos treated with BSA-loaded control beads, (**F-O**) Fgf8-loaded beads and (**P-W**) Bmp7-loaded beads; untreated sides of the embryos on the left, treated sides on the right, orientation as in Fig. 3B-E. The embryos were double labelled as indicated. Normal expression domains are marked by arrows, downregulated expression by open arrowheads, upregulated expression by filled arrowheads. The position of the beads is marked by asterisks. Note that Fgf8 beads placed into the head mesoderm did not influence positional values of the hindbrain or the neural crest cells, as evidenced by the unperturbed expression of *Hoxa2* (F,G). However, Fgf8 downregulated the lateral rectus marker (H,I) and upregulated the mandibular arch muscle marker (L,M). Unlike neural tube-mesoderm separation experiments, however, *Myf5* expression was also downregulated (J,K), while *MyoR* was upregulated (N,O; compare with Fig. 5). Bmp7 dowregulated *Paraxis* in the region of the lateral rectus EOM (P,Q) and *Myf5* in the region of the lateral rectus and the mandibular arch muscles (R,S). *En2* expression was downregulated in the distal part of the mandibular arch but not proximally close to the bead (T,U). *MyoR* was also downregulated, most prominently in the distal region of the arch (V,W). Scale bars: 250 μm in Ai,Aiii; 100 μm in Aii,Aiv; 200 μm in B-U. di, diencephalon; endo, endoderm; fn, frontonasal Fgf8 signal in ventral forebrain and surface ectoderm; hy, hyoid arch; i, isthmus; m, midbrain; ma, mandibular arch; ov, otic vesicle; pchp, prechordal plate; r, rhombomere; V, trigeminal ganglion; VII, facial nerve.

hypomorph mouse mutants that succeed in gastrulation specific responses of the head mesoderm to the loss of the epithelial Fgf signal have been observed (Frank et al., 2002). This suggests that Fgf8 signals to the head mesoderm directly, simultaneously supporting branchial arch muscle development and opposing the neural tube/EOM system.

Besides the arches, Fgf8 is strongly expressed by the isthmus, signalling in a planar fashion to organise mid- and hindbrain (Irving and Mason, 2000). However, the mesoderm next to the isthmus does not express *En2*. Employing limb induction as well-established Fgf8 response assay, we found that the ability of the isthmus to signal to neighbouring mesoderm is limited. Thus, isthmic Fgf8 may not be available to the head mesoderm. It cannot be excluded, however, that further factors found in the mandibular arch environment but not at the isthmus are required to upregulate *En2*.

Role of Fgf8 and Bmp7 in the control of head muscle differentiation

When head mesoderm and neural tube were separated, muscle differentiation remained on course. However, Fgf8, in addition to its patterning role also influenced muscle differentiation: *MyoR*, a marker for proliferative, undifferentiated MAM muscle precursors (von Scheven et al., 2006) was upregulated by Fgf8 while *Myf5* was downregulated. Thus suggests that Fgf8, similar to its role in the trunk (Itoh et al., 1996; Kahane et al., 2001), may expand the pool of muscle precursor in the head and may underpin muscle growth.

In contrast to Fgf8, Bmp7 strongly downregulated *Myf5*, and more mildly, *MyoR*. Thus, Bmp7 may inhibit the entry of head muscle precursors into any myogenic programmes. It has to be taken into account, however, that branchial arch mesoderm not only contributes to skeletal muscle but also to the anterior heart field and subsequently to the outflow tract of the heart (Kelly, 2005). Bmp molecules are important regulators of heart development (Brand, 2003). Hence it is possible that Bmp7 acted on the branchial arch mesoderm, diverting it from a skeletal muscle to a cardiac fate.

Eye muscle specification may be a prerequisite for the target recognition of the cognate nerves

When the head mesoderm was separated from the neural tube, leading to erroneous expression of *En2* in the muscle normally expressing *Paraxis* and *Lbx1*, then the abducens nerve destined for this muscle fell short of its target. Moreover, the nerve defasciculated, indicating that the axons struggled to identify their target and hence were actively sampling the environment (Tosney and Landmesser, 1985). When instead of the impermeable foil barrier, the filter was used, then marker gene expression and innervation of the lateral rectus was restored. This indicates that the progress of axonal outgrowth and target recognition was not hindered by the obstacle in its path. Rather, the innervation phenotype was linked to the presence of *Paraxis*/*Lbx1* or the absence of *En2* or both. This suggests that the neural tube specifies the eye muscle to aid its innervation. However, as *Paraxis*, *Lbx1* and *En2* are all transcription factors, we can expect that ultimately, the specification of the lateral rectus EOM leads to the production of cell surface or soluble axon guidance cues.

The abducens-lateral rectus pair is one of the rare examples of nerve and muscle not originating from the same axial level: the abducens nerve is born in rhombomeres 5 and 6; the lateral rectus muscle develops next to rhombomere 2 (Wahl et al., 1994). Moreover, it is only at rhombomere 2 levels that eye and branchiomeric muscles develop side by side (Couly et al., 1992; Noden, 1983a; Wachtler and Jacob, 1986). Furthermore, this region is traversed by a number of cranial nerves, with the abducens nerve arriving from posterior regions, the oculomotor nerve arriving from anterior regions and the maxillo-mandibular branch of the trigeminal projecting laterally into the mandibular arch (Chilton and Guthrie, 2004; Wahl et al., 1994). Thus, is it possible that signalling events and marker gene expression serve a unique function in head muscle development in this region. However, Fgf8 as signal to specify MAM is expressed in all branchial arches, and in hypomorph Fgf8 mouse mutants, severe pharyngeal and aortic arch defects were observed (Abu-Issa et al., 2002; Frank et al., 2002) (reviewed in Helms et al., 2005). Thus, it is likely that the neural tube-Fgf8/arch antagonism is a global regulator of eye versus branchiomeric muscle development.

Model

Summarising our results (Fig. 10), we propose that at a soluble signal from the neural tube (green), together with a further factor, specifies the neighbouring muscle anlage as *Paraxis/Lbx1*-positive lateral rectus EOM (yellow). Simultaneously these signals prevent the expression of the MAM marker *En2*. The correct specification of the lateral rectus then facilitates the innervation by the abducens nerve. Within the branchial arches, however, the presence of Fgf8

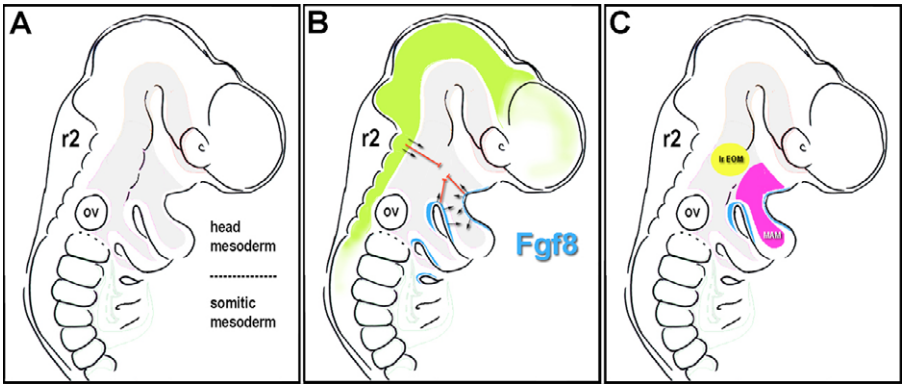

Fig. 10. Model for the specification of the lateral rectus eye versus mandibular arch muscles. (**A**) Schematic representation of a chick head at the onset of EOM and MAM-specific marker gene expression; the non-somitic head mesoderm is depicted in grey. (**B**) Factors from the neural tube (green) and Fgf8 from the branchial arches (blue) signal to the neighbouring head mesoderm. The signal from the neural tube is accompanied by a further, unidentified signal. As a result of the signalling events (**C**), the lateral rectus EOM anlage (yellow) is specified next to the neural tube; MAM markers are repressed in this area. MAM (magenta) are specified next to the mandibular Fgf8 signals that suppress EOM markers. lr EOM, lateral rectus extraocular muscle, MAM, mandibular arch muscles.

(blue) ensures that EOM markers are repressed while MAM markers (magenta) are supported. Thus, the neural tube derived signal and Fgf8 act antagonistically in head muscle specification. Yet, Fgf8 has an additional role in preventing MAM differentiation, maintaining the cells in a proliferative state.

We are most grateful to Frank Schubert, Lynda Erskine and Sarah Guthrie for helpful comments and to Frank Schubert for critically reading the manuscript. We also thank A. Graham, T. Lints, C. Logan, I. Mason, E. Olson and B. Patterson for kindly providing in-situ probes. The work was supported by the Charitable Foundation of Guy's Hospital, the Human Frontier Science Program and the European Network of Excellence, Myores. Gudrun von Scheven is an EU Marie Curie Early Stage Fellow.

Supplementary material

Supplementary material for this article is available at
http://dev.biologists.org/cgi/content/full/133/14/2731/DC1

References

Abu-Issa, R., Smyth, G., Smoak, I., Yamamura, K. and Meyers, E. N. (2002). Fgf8 is required for pharyngeal arch and cardiovascular development in the mouse. *Development* **129**, 4613-4625.
Alvares, L. E., Schubert, F. R., Thorpe, C., Mootoosamy, R. C., Cheng, L., Parkyn, G., Lumsden, A. and Dietrich, S. (2003). Intrinsic, Hox-dependent cues determine the fate of skeletal muscle precursors. *Dev. Cell* **5**, 379-390.
Begbie, J., Brunet, J. F., Rubenstein, J. L. and Graham, A. (1999). Induction of the epibranchial placodes. *Development* **126**, 895-902.
Bell, E., Wingate, R. J. and Lumsden, A. (1999). Homeotic transformation of rhombomere identity after localized Hoxb1 misexpression. *Science* **284**, 2168-2171.
Brand, T. (2003). Heart development: molecular insights into cardiac specification and early morphogenesis. *Dev. Biol.* **258**, 1-19.
Brent, A. E. and Tabin, C. J. (2002). Developmental regulation of somite derivatives: muscle, cartilage and tendon. *Curr. Opin. Genet. Dev.* **12**, 548-557.
Brodal, A. and Ragnar, F. (1963). *The Biology of Myxine*. Oslo: Grondahl & Son.
Cheng, L., Alvares, L. E., Ahmed, M. U., El-Hanfy, A. S. and Dietrich, S. (2004). The epaxial-hypaxial subdivision of the avian somite. *Dev. Biol.* **274**, 348-369.
Chilton, J. K. and Guthrie, S. (2004). Development of oculomotor axon projections in the chick embryo. *J. Comp. Neurol.* **472**, 308-317.
Cohn, M. J., Izpisua-Belmonte, J. C., Abud, H., Heath, J. K. and Tickle, C. (1995). Fibroblast growth factors induce additional limb development from the flank of chick embryos. *Cell* **80**, 739-746.
Couly, G. F., Coltey, P. M. and Le Douarin, N. M. (1992). The developmental fate of the cephalic mesoderm in quail-chick chimeras. *Development* **114**, 1-15.
Couly, G. F., Coltey, P. M. and Le Douarin, N. M. (1993). The triple origin of skull in higher vertebrates: a study in quail-chick chimeras. *Development* **117**, 409-429.
Dietrich, S., Schubert, F. R. and Lumsden, A. (1997). Control of dorsoventral pattern in the chick paraxial mesoderm. *Development* **124**, 3895-3908.
Dietrich, S., Schubert, F. R., Healy, C., Sharpe, P. T. and Lumsden, A. (1998). Specification of the hypaxial musculature. *Development* **125**, 2235-2249.
Engle, E. C. (2002). Applications of molecular genetics to the understanding of congenital ocular motility disorders. *Ann. N. Y. Acad. Sci.* **956**, 55-63.
Fan, C. M. and Tessier-Lavigne, M. (1994). Patterning of mammalian somites by surface ectoderm and notochord: evidence for sclerotome induction by a hedgehog homolog. *Cell* **79**, 1175-1186.
Fan, C. M., Lee, C. S. and Tessier-Lavigne, M. (1997). A role for WNT proteins in induction of dermomyotome. *Dev. Biol.* **191**, 160-165.
Ferrari, D., Sumoy, L., Gannon, J., Sun, H., Brown, A. M., Upholt, W. B. and Kosher, R. A. (1995). The expression pattern of the Distal-less homeobox-containing gene Dlx-5 in the developing chick limb bud suggests its involvement in apical ectodermal ridge activity, pattern formation, and cartilage differentiation. *Mech. Dev.* **52**, 257-264.
Frank, D. U., Fotheringham, L. K., Brewer, J. A., Muglia, L. J., Tristani-Firouzi, M., Capecchi, M. R. and Moon, A. M. (2002). An Fgf8 mouse mutant phenocopies human 22q11 deletion syndrome. *Development* **129**, 4591-4603.
Gage, P. J., Suh, H. and Camper, S. A. (1999). Dosage requirement of Pitx2 for development of multiple organs. *Development* **126**, 4643-4651.
Gans, C. and Northcutt, R. G. (1983). Neural crest and the origin of vertebrates: a new head. *Science* **220**, 268-274.
Gardner, C. A. and Barald, K. F. (1992). Expression patterns of engrailed-like proteins in the chick embryo. *Dev. Dyn.* **193**, 370-388.
Goodrich, E. S. (1958). *Studies on the Structure and Development of Vertebrates*. New York: Dover Publications.
Grammatopoulos, G. A., Bell, E., Toole, L., Lumsden, A. and Tucker, A. S. (2000). Homeotic transformation of branchial arch identity after Hoxa2 overexpression. *Development* **127**, 5355-5365.
Guthrie, S. and Lumsden, A. (1992). Motor neuron pathfinding following rhombomere reversals in the chick embryo hindbrain. *Development* **114**, 663-673.
Hacker, A. and Guthrie, S. (1998). A distinct developmental programme for the cranial paraxial mesoderm in the chick embryo. *Development* **125**, 3461-3472.
Hadchouel, J., Tajbakhsh, S., Primig, M., Chang, T. H., Daubas, P., Rocancourt, D. and Buckingham, M. (2000). Modular long-range regulation of Myf5 reveals unexpected heterogeneity between skeletal muscles in the mouse embryo. *Development* **127**, 4455-4467.
Hamburger, V. and Hamilton, H. L. (1951). A series of normal stages in the development of the chick embryo. *J. Morph.* **88**, 49-92.
Helms, J. A., Cordero, D. and Tapadia, M. D. (2005). New insights into craniofacial morphogenesis. *Development* **132**, 851-861.
Hernandez, R. E., Rikhof, H. A., Bachmann, R. and Moens, C. B. (2004). vhnf1 integrates global RA patterning and local FGF signals to direct posterior hindbrain development in zebrafish. *Development* **131**, 4511-4520.
Hippenmeyer, S., Kramer, I. and Arber, S. (2004). Control of neuronal phenotype: what targets tell the cell bodies. *Trends Neurosci.* **27**, 482-488.
Irving, C. and Mason, I. (2000). Signalling by FGF8 from the isthmus patterns anterior hindbrain and establishes the anterior limit of Hox gene expression. *Development* **127**, 177-186.
Itoh, N., Mima, T. and Mikawa, T. (1996). Loss of fibroblast growth factor receptors is necessary for terminal differentiation of embryonic limb muscle. *Development* **122**, 291-300.

Jacob, J., Hacker, A. and Guthrie, S. (2001). Mechanisms and molecules in motor neuron specification and axon pathfinding. *BioEssays* **23**, 582-595.
Jacob, M., Jacob, H. J., Wachtler, F. and Christ, B. (1984). Ontogeny of avian extrinsic ocular muscles. I. A light- and electron-microscopic study. *Cell Tissue Res.* **237**, 549-557.
Johnson, R. L., Laufer, E., Riddle, R. D. and Tabin, C. (1994). Ectopic expression of Sonic hedgehog alters dorsal-ventral patterning of somites. *Cell* **79**, 1165-1173.
Kahane, N., Cinnamon, Y., Bachelet, I. and Kalcheim, C. (2001). The third wave of myotome colonization by mitotically competent progenitors: regulating the balance between differentiation and proliferation during muscle development. *Development* **128**, 2187-2198.
Kardon, G. (1998). Muscle and tendon morphogenesis in the avian hind limb. *Development* **125**, 4019-4032.
Kelly, R. G. (2005). Molecular inroads into the anterior heart field. *Trends Cardiovasc. Med.* **15**, 51-56.
Kelly, R. G., Jerome-Majewska, L. A. and Papaioannou, V. E. (2004). The del22q11.2 candidate gene Tbx1 regulates branchiomeric myogenesis. *Hum. Mol. Genet.* **13**, 2829-2840.
Kitamura, K., Miura, H., Miyagawa-Tomita, S., Yanazawa, M., Katoh-Fukui, Y., Suzuki, R., Ohuchi, H., Suehiro, A., Motegi, Y., Nakahara, Y. et al. (1999). Mouse Pitx2 deficiency leads to anomalies of the ventral body wall, heart, extra- and periocular mesoderm and right pulmonary isomerism. *Development* **126**, 5749-5758.
Köntges, G. and Lumsden, A. (1996). Rhombencephalic neural crest segmentation is preserved throughout craniofacial ontogeny. *Development* **122**, 3229-3242.
Logan, C., Hanks, M. C., Noble-Topham, S., Nallainathan, D., Provart, N. J. and Joyner, A. L. (1992). Cloning and sequence comparison of the mouse, human, and chicken engrailed genes reveal potential functional domains and regulatory regions. *Dev. Genet.* **13**, 345-358.
Lours, C. and Dietrich, S. (2005). The dissociation of the Fgf-feedback loop controls the limbless state of the neck. *Development* **132**, 5553-5564.
Lu, J. R., Bassel-Duby, R., Hawkins, A., Chang, P., Valdez, R., Wu, H., Gan, L., Shelton, J. M., Richardson, J. A. and Olson, E. N. (2002). Control of facial muscle development by MyoR and capsulin. *Science* **298**, 2378-2381.
Lumsden, A., Sprawson, N. and Graham, A. (1991). Segmental origin and migration of neural crest cells in the hindbrain region of the chick embryo. *Development* **113**, 1281-1291.
Mahmood, R., Bresnick, J., Hornbruch, A., Mahony, C., Morton, N., Colquhoun, K., Martin, P., Lumsden, A., Dickson, C. and Mason, I. (1995). A role for FGF-8 in the initiation and maintenance of vertebrate limb bud outgrowth. *Curr. Biol.* **5**, 797-806.
Moens, C. B., Cordes, S. P., Giorgianni, M. W., Barsh, G. S. and Kimmel, C. B. (1998). Equivalence in the genetic control of hindbrain segmentation in fish and mouse. *Development* **125**, 381-391.
Mootoosamy, R. C. and Dietrich, S. (2002). Distinct regulatory cascades for head and trunk myogenesis. *Development* **129**, 573-583.
Münsterberg, A. E., Kitajewski, J., Bumcrot, D. A., McMahon, A. P. and Lassar, A. B. (1995). Combinatorial signaling by Sonic hedgehog and Wnt family members induces myogenic bHLH gene expression in the somite. *Genes Dev.* **9**, 2911-2922.
Nakano, M., Yamada, K., Fain, J., Sener, E. C., Selleck, C. J., Awad, A. H., Zwaan, J., Mullaney, P. B., Bosley, T. M. and Engle, E. C. (2001). Homozygous mutations in ARIX(PHOX2A) result in congenital fibrosis of the extraocular muscles type 2. *Nat. Genet.* **29**, 315-320.
Noden, D. M. (1983a). The embryonic origins of avian cephalic and cervical muscles and associated connective tissues. *Am. J. Anat.* **168**, 257-276.
Noden, D. M. (1983b). The role of the neural crest in patterning of avian cranial skeletal, connective, and muscle tissues. *Dev. Biol.* **96**, 144-165.
Noden, D. M., Marcucio, R., Borycki, A. G. and Emerson, C. P., Jr (1999). Differentiation of avian craniofacial muscles: I. Patterns of early regulatory gene expression and myosin heavy chain synthesis. *Dev. Dyn.* **216**, 96-112.
Parkyn, G., Mootoosamy, R. C., Cheng, L., Thorpe, C. and Dietrich, S. (2002). Hypaxial muscle development. *Results Probl. Cell Differ.* **38**, 127-141.
Pasqualetti, M., Ori, M., Nardi, I. and Rijli, F. M. (2000). Ectopic Hoxa2 induction after neural crest migration results in homeosis of jaw elements in Xenopus. *Development* **127**, 5367-5378.
Paterson, J. A. and Kaiserman-Abramof, I. R. (1981). The oculomotor nucleus and extraocular muscles in a mutant anophthalmic mouse. *Anat. Rec.* **200**, 239-251.
Pun, S., Sigrist, M., Santos, A. F., Ruegg, M. A., Sanes, J. R., Jessell, T. M., Arber, S. and Caroni, P. (2002). An intrinsic distinction in neuromuscular junction assembly and maintenance in different skeletal muscles. *Neuron* **34**, 357-370.
Saitoh, O., Fujisawa-Sehara, A., Nabeshima, Y. and Periasamy, M. (1993). Expression of myogenic factors in denervated chicken breast muscle: isolation of the chicken Myf5 gene. *Nucleic Acids Res.* **21**, 2503-2509.
Schilling, T. F., Walker, C. and Kimmel, C. B. (1996). The chinless mutation and neural crest cell interactions in zebrafish jaw development. *Development* **122**, 1417-1426.
Schubert, F. R. and Lumsden, A. (2005). Transcriptional control of early tract formation in the embryonic chick midbrain. *Development* **132**, 1785-1793.
Sosic, D., Brand-Saberi, B., Schmidt, C., Christ, B. and Olson, E. N. (1997). Regulation of paraxis expression and somite formation by ectoderm- and neural tube-derived signals. *Dev. Biol.* **185**, 229-243.
Summerbell, D., Ashby, P. R., Coutelle, O., Cox, D., Yee, S. and Rigby, P. W. (2000). The expression of Myf5 in the developing mouse embryo is controlled by discrete and dispersed enhancers specific for particular populations of skeletal muscle precursors. *Development* **127**, 3745-3757.
Tosney, K. W. and Landmesser, L. T. (1985). Growth cone morphology and trajectory in the lumbosacral region of the chick embryo. *J. Neurosci.* **5**, 2345-2358.
Trainor, P. and Krumlauf, R. (2000). Plasticity in mouse neural crest cells reveals a new patterning role for cranial mesoderm. *Nat. Cell Biol.* **2**, 96-102.
Tzahor, E., Kempf, H., Mootoosamy, R. C., Poon, A. C., Abzhanov, A., Tabin, C. J., Dietrich, S. and Lassar, A. B. (2003). Antagonists of Wnt and BMP signaling promote the formation of vertebrate head muscle. *Genes Dev.* **17**, 3087-3099.
Veitch, E., Begbie, J., Schilling, T. F., Smith, M. M. and Graham, A. (1999). Pharyngeal arch patterning in the absence of neural crest. *Curr. Biol.* **9**, 1481-1484.
Vitelli, F., Morishima, M., Taddei, I., Lindsay, E. A. and Baldini, A. (2002a). Tbx1 mutation causes multiple cardiovascular defects and disrupts neural crest and cranial nerve migratory pathways. *Hum. Mol. Genet.* **11**, 915-922.
Vitelli, F., Taddei, I., Morishima, M., Meyers, E. N., Lindsay, E. A. and Baldini, A. (2002b). A genetic link between Tbx1 and fibroblast growth factor signaling. *Development* **129**, 4605-4611.
von Scheven, G., Bothe, I., Ahmed, M. U., Alvares, L. E. and Dietrich, S. (2006). Protein and genomic organisation of vertebrate MyoR and Capsulin genes and their expression during avian development. *Gene Expr. Patterns* **6**, 383-393.
Wachtler, F. and Jacob, M. (1986). Origin and development of the cranial skeletal muscles. *Bibl. Anat.* **29**, 24-46.
Wahl, C. M., Noden, D. M. and Baker, R. (1994). Developmental relations between sixth nerve motor neurons and their targets in the chick embryo. *Dev. Dyn.* **201**, 191-202.